Electronic Supplementary Information

Synergistic Effect of Hierarchical Nanopores in Co-doped cobalt oxides 3D Flowers for Electrochemical Energy Storage

Xia Deng,[1‡] Hong Zhang,[2‡] Junwei Zhang,[2] Dongsheng Lei[2] and Yong Peng*[2]

[1]School of Life Sciences, Electron Microscopy Center of Lanzhou University, Lanzhou, 730000, P. R. China

[2]Electron Microscopy Centre of Lanzhou University, Key Laboratory of Magnetism and Magnetic Materials of the Ministry of Education and School of Physical Science and Technology, Lanzhou University, Lanzhou 730000, P. R. China.

[‡]These authors equally contributed to this work.

E-mail: pengy@lzu.edu.cn

This file contains Supplementary Scheme 1, Tabel S1, Figures S1, S2, S3, S4, S5, S6, S7.

Formation mechanism of precursor $Co(OH)_2$ 3DFs

The different morphologies of $Co(OH)_2$ are tailored by the dissociation rates of the ethanolamine based on different concentrations. The concentration plays a key role in the kinetic reaction of counter ions of Co^{2+} and dissociated OH^-. Small nuclei will be created at the sites of initial $Co(OH)_2$ suspensions, and followed by aggregation/self-assembly into larger particles/structures with a particular morphology, which is driven by the force to minimize the surface energy. The pink precipitates which began to appear at the bottom of the glass vial after 6 h (with 15 ml theethanolamine) were

investigated by SEM, showing a 3DF morphology. It reveals that the process of nucleation is very slow and the process of growth and aggregation/self-assembly into 3DFs is very fast, showing a slow nucleation and fast growth mechanism. At low OH^- concentration, there is a relatively smaller number of nuclei and a sufficient time and room for particle growth. This leads to the formation of more petals and larger size flower-liked 3D $Co(OH)_2$ ($Co(OH)_2$ 3DFs), while the energetically favored state is clarified by the Ostwald ripening process.[1-2] On the other hand, at high OH^- concentration, a larger number of nuclei were created and there remained relatively limited Co^{2+} in the reaction solution, which future grew into a less petal and smaller size $Co(OH)_2$ 3DFs.

The assumption of the plausible reaction pathways for the transformation mechanism is as following: the β-$Co(OH)_2$ nanosheets synthesized used this method are not stable under heating, easily transformed to Co_3O_4 crystals. During the calcined in an Ar environment, the Ar crashed the Co_3O_4 crystal and took out the O^{2-} ion producing O vacancies.[3-4] Then the Co_3O_4 could be decomposed into CoO[5] or even Co. Subsequently, Co_3O_4/CoO/Co composites were steered by Kirkendall Effect, which can take place in the matal/metal oxide system.[6] When the reaction front localized at the Co/Co_3O_4 or Co/CoO composites interface, the reduced Co metallic ions diffuse through outward the growing Co_3O_4/CoO composites nanosheets aggregate into nanoparticles and generate a nanopore inside the Co_3O_4/CoO composites,[7] forming the hierarchically nanoporous Co/Co_3O_4-CoO nanostructure.

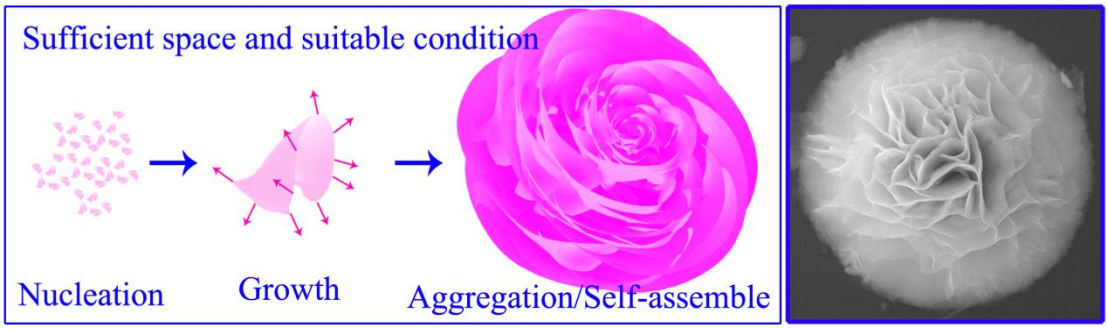

Scheme 1 Schematic diagram showing the formation mechanism of $Co(OH)_2$ 3DFs and the corresponding SEM image.

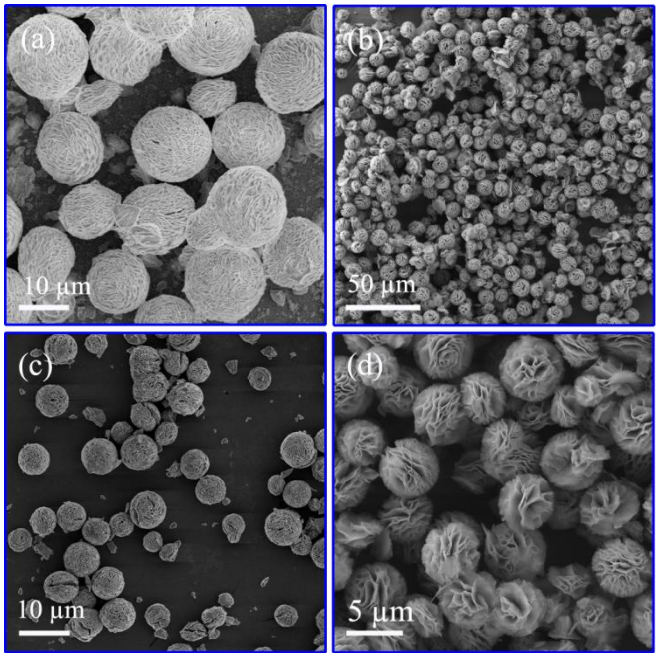

Figure S1 The calcination precursors β-$Co(OH)_2$ 3DFs, which are perpared with different stoichiometry of theethanolamine: (a) 10 ml (named as CH1), (b) 20 ml (named as CH2), and their corresponding calcined samples, Co/Co_3O_4-CoO 3DFs, as shown in (c) C1 and (d) C2.

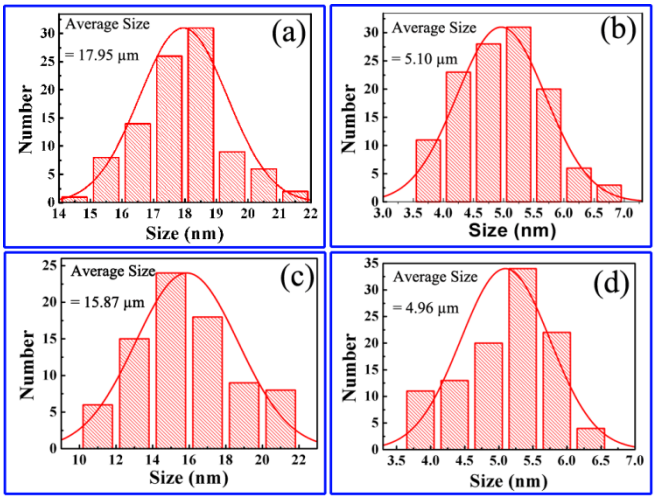

Figure S2 The size distributions of the precursors β-$Co(OH)_2$ 3DFs: (a) CH1 speciment; (b) CH2 specimen; (c) and (d) their corresponding calcined Co/Co_3O_4-CoO 3DFs, respectively.

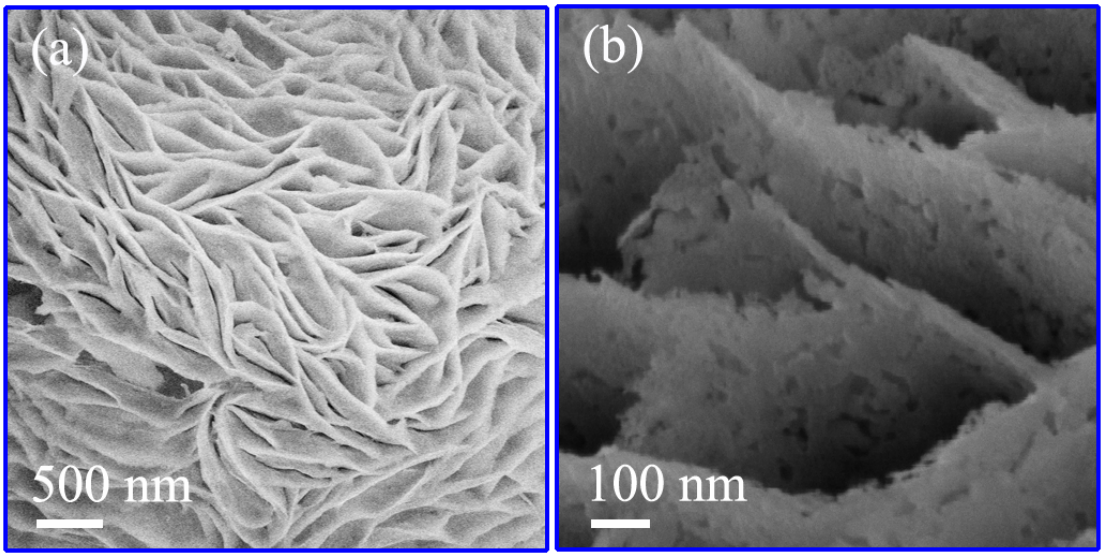

Figure S3 The SEM images of the morphologies of the nanosheets of (a) the β-$Co(OH)_2$ 3DFs (CH1) and (b) the Co/Co_3O_4-CoO 3DFs (C1).

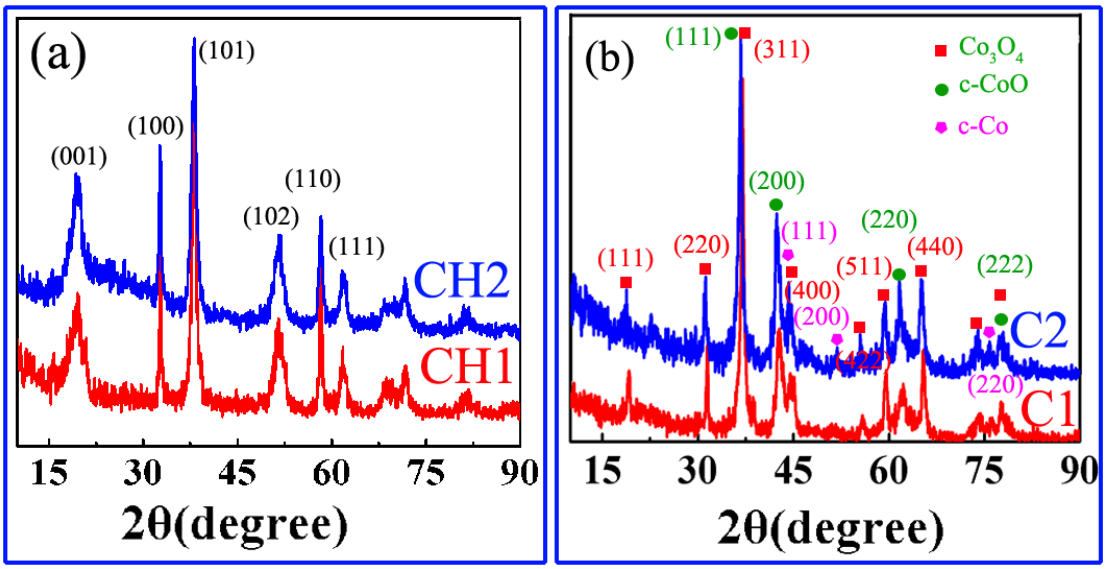

Figure S4 (a) XRD spectra of precursors β-$Co(OH)_2$ 3DFs (red for CH1 specimen and blue for CH2); (b) XRD spectra of the corresponding calcined Co/Co_3O_4-CoO 3DFs (red for C1 and blue for C2).

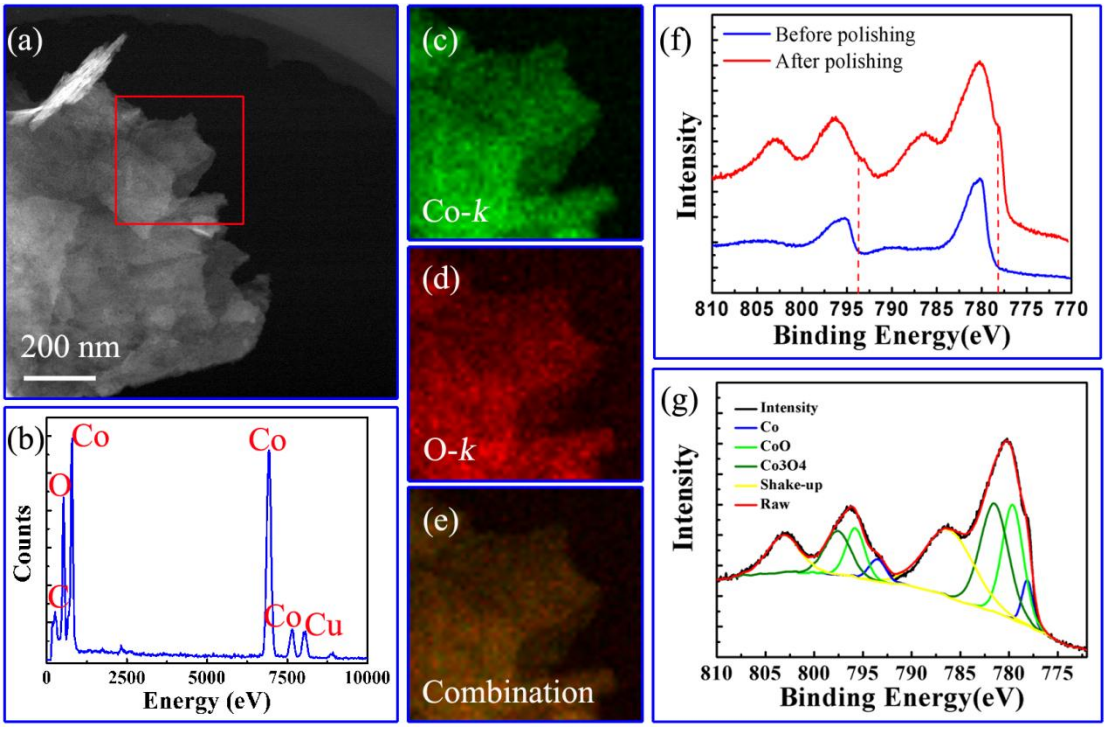

Figure S5 Chemical characterization of the uniformly nanoporous Co-Co_3O_4-CoO 3DFs (specimen C2): (a) HAADF-STEM image of the nanosheets used for elemental

mapping analysis; (b) EDX spectrum; (c) cobalt mapping; (d) oxygen mapping; (e) their combination; (f) XPS spectra before and after polishing; (g) the fitted XPS spectra after polishing.

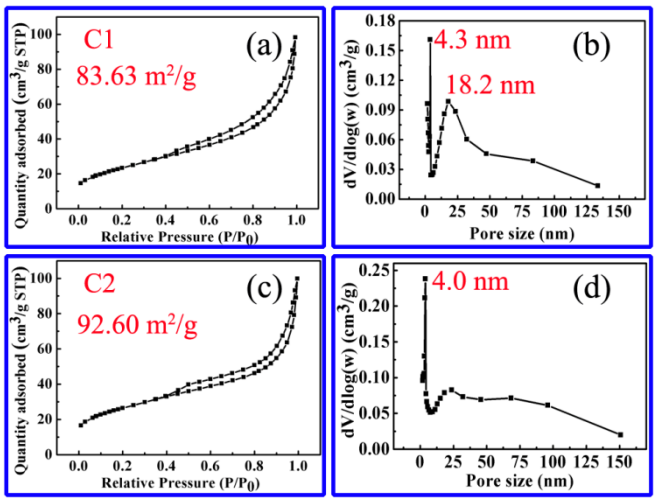

Figure S6 (a) Nitrogen (N_2) adsorption-desorption isotherm of the hierarchically nanoporous Co/Co_3O_4-CoO 3DFs (C1) and (b) the corresponding pore size distribution; (c) Nitrogen (N2) adsorption-desorption isotherm of the uniformly nanoporous Co/Co_3O_4-CoO 3DFs (C2) and (d) the corresponding pore size distribution.

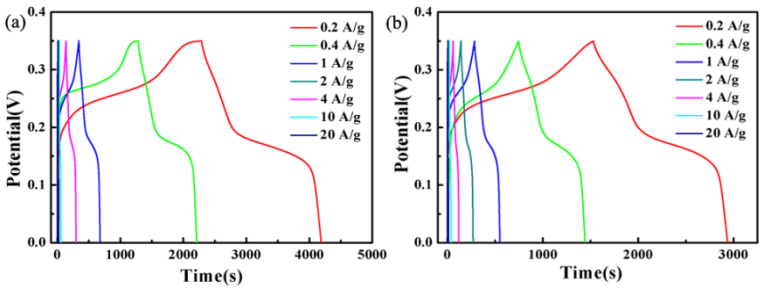

Figure S7 Galvanostatic charge/discharge curves of the hierarchically nanoporous Co/Co_3O_4-CoO 3DFs (a) and uniformly nanoporous Co/Co_3O_4-CoO 3DFs (b) at different current densities.

Tabel S1 The comparision of the performance of nanoporous Co/Co_3O_4-CoO 3DFs and other electrolyte materials

Electrode materials	Specific capacitance(F/g)	Current density(A/g)	Ref
Co_3O_4	604	4	16
CoO/Co_3O_4	362.8	0.2	47
Co_3O_4	599	2	64
Co_3O_4	358	2	65
Co_3O_4	754	2	66
Co_3O_4 on rGO/CNTs	378	2	67
Co_3O_4 - CNFs	556	1	68
Co_3O_4	150	1	69
Co_3O_4	401	0.5	70
CoO	600	0.5	71
a-CoMoO4	90	2	72
CoO	311.8	1	73
CoMoO4	380	1	74
Co/Co_3O_4-CoO 3DFs	902.3	1	This work

Reference

[1] A. M. Cao, J. S. Hu, H. P. Liang, W. G. Song, L. J. Wan, X. L. He, X. G. Gao, S. H. Xia, *J. Phys. Chem. B*, 2006, **110**, 15858-15863.

[2] C. Mondal, M. Ganguly, P. K. Manna, S. M. Yusuf, T. Pal, *Langmuir*, 2013, **29**, 9179−9187.

[3] D. Q. Gao, G. J. Yang, J. Y. Li, J. Zhang, J. J. Zhang, D. S. Xue, *J. Phys. Chem. C*, 2010, **114**, 18347–18351.

[4] G. J. Yang, D. Q. Qiang, Z. H. Shi, Z. H. Zhang, J. Zhang, J. L. Zhang, D. S. Xue, *J. Phys. Chem. C*, 2010, **114**, 21989–21993.

[5] L. Liao, Q. H. Zhang, Z. H, Su, Z. Z. Zhao, Y. N. Wang, Y. Li, X. X. Lu, D. G. Wei, G. Y. Feng, Q. K. Yu, X. J. Cai, I. M. Zhao, Z. F. Ren, H. Fang, F. Robles-Hernandez, S. Baldelli, J. M. Bao, *Nature Nanotech.,* 2014, **9**, 69-73.

[6] A. A. E. Mel, L. M. Luna, M. Buffière, P. Y. Tessier, K. Du, C. H. Choi, H. J. Kleebe, S. Konstantinidis, C. Bittencourt, R. Snyders, *ACS Nano*, 2014, **8**, 1854-1861.

[7] A. Cabot, M. Ibáñez, P. Guardia, A. P. Alivisatos, *J. Am. Chem. Soc.,* 2009, **131**, 11326-11328.